

# DoMCoSAR: A Novel Approach for Establishing the Docking Mode That Is Consistent with the Structure–Activity Relationship. Application to HIV-1 Protease Inhibitors and VEGF Receptor Tyrosine Kinase Inhibitors

Michal Vieth\* and David J. Cummins

Eli Lilly and Company, Lilly Research Laboratories, Lilly Corporate Center, DC 1513, Indianapolis, Indiana 46285

Received December 14, 1999

DoMCoSAR is a novel approach for statistically determining the docking mode that is consistent with a structure–activity relationship. The approach establishes the binding mode for the compounds in a chemical series with the assumption that all molecules exhibit the same binding mode. It involves three stages. In the first stage all molecules that belong to a given chemical series are docked to the active site of the protein target. The only bias used in the docking at this stage involves the location of the protein binding site. Coordinates of the common substructure (CS) that results from the unbiased docking are then clustered to establish the major substructure docking modes. In the second stage all molecules are docked to the major docking modes (MDMs) with constraints based on the common substructure. The third stage generates, for the major docking modes, interaction-based descriptors that include electrostatic, VDW, strain, and solvation contributions. The problem of docking mode evaluation is now reduced to the question of which descriptor set is more predictive. To establish a quantitative comparison of the descriptor sets associated with the major docking modes, we use 50 instances of random 4-fold cross-validation. For each 4-fold cross-validation the predictive squared correlation coefficient ( $R^2$ ) is computed. *t*-Tests are applied to establish significance of the differences in mean  $R^2$  for one docking mode versus another. We test the methodology on two test cases: HIV-1 protease inhibitors (Holloway et al. *J. Med. Chem.* **1995**, *38*, 305–317) and vascular endothelial growth factor (VEGF) receptor tyrosine kinase oxindoles (Sun et al. *J. Med. Chem.* **1998**, *41*, 2588–2603). For both test cases there is statistically significant preference for the binding mode consistent with the X-ray structure. The appeal of this methodology is that researchers gain the objectivity of statistical justification for the selected docking mode. The methodology is relatively insensitive to subtle variations of the protein structure that include, but are not limited to, side chain and small backbone rearrangement during binding. In addition, predictive models that result from the approach can be used to further optimize chemical series.

## Introduction

High-throughput screening (HTS) of combinatorial and corporate libraries allows for screening thousands of compounds in a short period of time.<sup>3,4</sup> Even though HTS techniques have been developed and fully implemented at many pharmaceutical companies around the world, there is a finite cost associated with the screening of each compound. Thus for some selected targets screening smaller, biased libraries of compounds may prove beneficial.<sup>5</sup> A popular technique for reducing a library of molecules to a manageable size is rapid docking and scoring,<sup>6–8</sup> also known as structure-based virtual screening. The popularity of this approach can be inferred from the fact that the principles of structure-based screening date back to the late 19th century with Fisher's concept of the lock-and-key mechanism of enzyme action.<sup>9</sup> It is believed that limiting a library to molecules that fit and complement the receptor active site should improve the rate at which the hits are identified. Although appealing, the methodology of rapid docking and scoring has not been properly evaluated and the limitations and pitfalls have not been addressed.

Another application of computer docking methodology is optimization of lead molecules. In many cases an X-ray structure of the target is available or a homology model can be produced. Docking techniques allow for placement of the lead molecule in the context of the receptor active site,<sup>10,11</sup> and in some cases new synthetic directions emerge for improving the potency (or other characteristics) of a given lead series.<sup>1</sup> In addition, docking of compounds from a lead series can be helpful in creation of predictive quantitative structure–activity relationship (QSAR) models.<sup>1,12,13</sup> These models can be used to prioritize synthesis of compounds and quantitatively evaluate potential modifications of the lead series.

Most available docking algorithms meet a minimum standard of being able to reproduce orientations of the protein–ligand X-ray structures.<sup>14–17</sup> In the majority of real life problems, however, the exact structure of the protein from the complex is not a priori available. Binding of highly similar ligands can cause minor or, in the case of protein kinases, quite substantial rearrangements of the protein.<sup>18,19</sup> Prediction of protein rearrangements upon binding is a problem similar to predicting structural changes observed between homologous proteins. According to CASP3 competition results, current methods are not able to deal effectively with this

\* To whom correspondence should be addressed. Phone: (317) 277-3959. Fax: (317) 276-6545. E-mail: m.vieth@lilly.com.

problem.<sup>20,21</sup> Despite a frequent inability to predict structural changes upon binding, chemical changes in a series of potent ligands may be able to aid in the selection of the docking mode.

This paper addresses the goal of obtaining a docking mode that is consistent with the structure–activity relationship (SAR). We introduce a methodology that allows a medicinal chemist to choose a docking solution that is consistent with the observed activity of a series of ligands. In addition some potential pitfalls associated with utilizing homology models for prediction are highlighted. Finally, the results of fully automated models are contrasted with models involving some manual intervention.

## Materials and Methods

The docking protocol utilizes a combination of simulated annealing and CHARMM<sup>22</sup>-based energy function and is described in detail elsewhere.<sup>14,23</sup> For the sake of introduction we present a summary of the protocol. An initial random distribution of ligand replicas is generated around the active site. The docking protocol involving dynamics of ligand replicas consists of three stages. In the first stage, the energy surface is explored by annealing ligands starting at high temperatures with soft-core nonbonded interactions. In the second stage local minima are identified in the basins provided by the first stage. The soft core is gradually hardened, and the starting temperature for the annealing is decreased. In the last stage of the protocol the soft core potential disappears and the resulting structures are locally minimized. In this work the protocol is adjusted slightly, as described below.

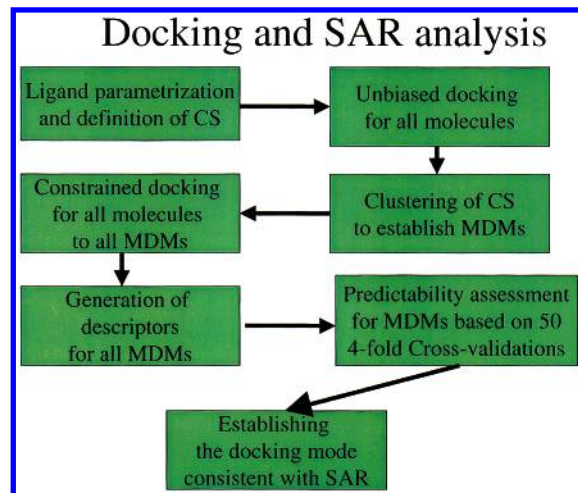
**Parameters and Docking Potential.** A previous study established that utilization of the soft core potential is essential for an efficient docking protocol. This work implements a different form of the soft core potential<sup>24</sup> to allow for physical characteristics of model systems such as SPC water dimer. This new soft core potential is defined independently for the electrostatic and van der Waals (VDW) components in the following way:

$$E_{ij} = E_{\max} - ar_{ij}^b \text{ if } E_{ij} > \frac{E_{\max}}{2} \quad (1)$$

otherwise the usual form for the nonbonded interactions is utilized.<sup>24</sup> The switching to the soft core potential occurs at the distance  $R_{\text{cut}}$  defined such that:

$$E_{ij}(R_{\text{cut}}) = E_{\max}/2 \quad (2)$$

The coefficients  $a$  and  $b$  are chosen so that the energy and force terms agree at  $R_{\text{cut}}$ . Note that for the electrostatic attraction both  $E_{\max}$  and  $a$  are negative. The qualitative and quantitative results for the docking on model systems remain unchanged for the test systems described in previous papers.<sup>14,23</sup> For the first heating stage of the docking protocol, a value of  $E_{\max}$  equal to 1.5, −10.0, and 20.0 is utilized for the VDW, electrostatic attraction, and repulsion terms, respectively. In the cooling stage the  $E_{\max}$  values are set to 3.0, −20.0, and 40.0. In the third stage the values are changed to 30, −200, and 400, and in the last stage the regular form of the potential is used. The polar hydrogen representation of the protein is used together with PARAM19/TOPI19 parameter and topology files.<sup>22</sup> All hydrogen ligand parameter files are created by Quanta98.<sup>25</sup> Ligand charges are generated by Gaussian94 with the HF/6-31G\* basis set.<sup>26</sup> For the HIV-1 protease inhibitor set we also use five other charge assignment methods available in InsightII for comparison purposes.<sup>27</sup> The ligand center of masses are restricted harmonically if their distance exceeds 6 Å from the center of the active site. The center of the active site is defined as the center of mass of the ligand from X-ray structure of the complex.



**Figure 1.** Schematic representation of the docking mode selection. First, the ligands are parametrized and a common substructure (CS) is defined for the series. Docking to the binding site for all molecules is performed followed by rms clustering of the resulting CS coordinates. The centers of significant clusters define the coordinates of the major docking modes (MDMs). All molecules are docked again with restraints so that the entire series is docked in a way corresponding to the MDMs. For each MDM, descriptors are generated based on the CHARMM force field. Each MDM will have a different corresponding descriptor set due to a different position of the series with respect to the receptor. Predictability of each descriptor set is assessed based on random 4-fold cross-validation performed 50 times. The most predictive descriptor set is chosen to indicate the docking mode that is most consistent with the SAR.

**Docking and Generation of Descriptors.** The assumption is made that all molecules in the chemical series adopt the same binding mode. This assumption allows for establishing the most probable binding mode for a series of compounds after extracting probable common substructure (CS) binding modes from unbiased docking experiments. It is especially important for docking to an imperfect protein model which could prevent some molecules, sometimes the most potent ones, from accessing the true binding due to steric changes caused frequently by side chain or small backbone rearrangements. Because of the assumption of common binding mode, DoMCoSAR is currently limited to congeneric chemical series and is not applicable to virtual screening of diverse sets of molecules. However, DoMCoSAR can be used with any docking approach including but not limited to DOCK,<sup>10</sup> AutoDock,<sup>17</sup> and GOLD<sup>16</sup> packages.

The entire procedure is schematically depicted in Figure 1. For each ligand, the experiment proceeds by randomly generating 20 replicas of ligands and annealing them following the protocol described in the previous papers.<sup>14,23</sup> The mean docking time for this stage of the studies is 12 min/replica on SGI 200Mhz R10000 chip. The ligand replicas are clustered to obtain the final solution for each molecule/ligand in the series. The clustering method used is a root mean square (rms)-based Ward's hierarchical, agglomerative clustering<sup>28</sup> applied only to the heavy atom coordinates. The clustering is carried out until the largest radius of the clusters is less than 1.5 Å.<sup>29</sup> The decision to choose a 1.5 Å cluster radius as the stopping criterion was arbitrary, but chosen such that cluster centers were consistent with visual interpretation of docking results.

CS of all final solutions for all ligands are subsequently clustered to obtain the major docking modes (MDM) for substructures. The major docking modes are usually populated by more than 40% of the ligands. Once the major docking modes are established, all ligands are redocked for each selected docking mode with restraints to the position of the substructure MDMs utilizing the short version of annealing



**Figure 2.** 4-Fold cross-validation scheme. The data set is randomly divided into four equal subsets. The activities of the molecules in each subset (test set) are predicted from a model trained on the activities of molecules for the remaining subsets (train set). The procedure yields predictions for all molecules. The random division of the molecules is repeated 50 times so that each time the test sets are different.

schedule.<sup>14</sup> For this stage of the protocol the mean redocking time is 3 min/replica on SGI 200Mhz R10000 chip. NOE distance restraints are employed between the CS atoms and the dummy atoms positioned at the MDM coordinates. A force constant of 20 kcal/Å<sup>2</sup> is used with  $R_{\text{max}} = 0.5$  Å. At this stage 4 ligand replicas are utilized rather than 20 as used in the initial docking. At the end of this stage the entire chemical series is positioned in the active site in a number of ways with CS occupying the positions corresponding to MDMs. For each MDM interaction energy descriptors are generated for the entire chemical series. Four structure-based descriptors were selected for building predictive models. Electrostatic ( $\text{eps} = 2r$ ) and VDW contributions to the interaction energy with the receptor were chosen, as well as the strain energy and the atom type weighted difference in total exposed surface area<sup>30</sup> between receptor and ligand in the complex and in the isolated state. The strain energy is defined as the difference between the internal energy in the docked conformation and the internal energy of the final ligand conformation that was extracted from the active site and minimized with 200 steps of conjugate gradient minimization.

At this stage each docking mode is represented by a set of descriptors. If one considers only two MDMs, the problem of selecting the one that is more consistent with the SAR reduces to the question: which descriptor set is more predictive? To answer this question a 4-fold cross-validation study is performed. A 4-fold cross-validation consists of dividing the entire set of molecules into four subsets at random. In each subset, the activity of each molecule is predicted from a (QSAR) model derived from the molecules in the three remaining subsets. Thus, four different models are built on four different training sets, each one of which is 75% of the size of the whole data set. In this way the activity of all molecules in the set is predicted (see Figure 2). 4-Fold cross-validation (especially repeated numerous times) gives a far more realistic estimate of the predictive power of the method than a leave-one-out test, since the 4-fold test predicts substantial fractions of "new" data and is less prone to giving misleading optimistic results if the data set contains pairs of identical or highly similar molecules. The method of partial least squares<sup>31,32</sup> is applied using the SAS system<sup>33</sup> to determine a set of regression coefficients for the training set of molecules:

$$y_k = \sum_{i=1}^N c_{ij} D_{ijk} \quad (3)$$

where  $y_k$  is the experimentally determined  $\text{pIC}_{50} = -\log(\text{IC}_{50})$

for the  $k$ th compound,  $k = 1 \dots K$  where  $K$  is the total size of the data set,  $c_{ij}$  is the contribution to the activity of the descriptor  $D_{ijk}$  for the  $j$ th binding mode in each of two latent variables, and  $N$  is the number of descriptors. In this study  $N = 4$  and the two best docking modes  $j = 1, 2$  are compared. Our measure of predictability is the squared predictive correlation coefficient  $R^2$  defined as:

$$R^2 = \frac{[\sum_{i=1}^K (y_i - \bar{y})(\hat{y}_i - \bar{\hat{y}})]^2}{\sum_{i=1}^K (y_i - \bar{y})^2 \sum_{i=1}^K (\hat{y}_i - \bar{\hat{y}})^2} \quad (4)$$

where  $\bar{y}$  is the mean of the observed  $\text{pIC}_{50}$ s,  $\hat{y}_i$  is the predicted  $\text{pIC}_{50}$  for the  $i$ th compound, and  $\bar{\hat{y}}$  is the mean predicted  $\text{pIC}_{50}$ .

Since there is a chance that a single data split is anecdotal, we perform 50 random 4-fold data splits, each time building a fresh set of predictive models. For visualization the distribution of the 50 resulting values of  $R^2$  is estimated using Normal kernel density estimation, where the optimal smoothing bandwidth is estimated by generalized cross-validation.<sup>34</sup> Thus, for each descriptor set corresponding to each docking mode we have a distribution of  $R^2$ . There are several statistics that are called  $R^2$ ,  $Q^2$ , etc.; the above formulation of  $R^2$  ranges from 0 (no correlation) to 1 (perfect correlation). One may examine the distributions and visually determine which one is better. However, if the distributions overlap it may be desirable to use an objective criterion to determine which descriptor set is on average more predictive. The  $t$ -test can be used to obtain  $p$ -values<sup>35</sup> for the differences in means of two distributions. The  $t$  statistic is defined by:

$$t^* = \frac{\bar{\hat{y}}_r - \bar{\hat{y}}_s}{\sqrt{\frac{\sum (\hat{y}_r - \bar{\hat{y}}_r)^2}{(K_r - 1)K_r} + \frac{\sum (\hat{y}_s - \bar{\hat{y}}_s)^2}{(K_s - 1)K_s}}} \quad (5)$$

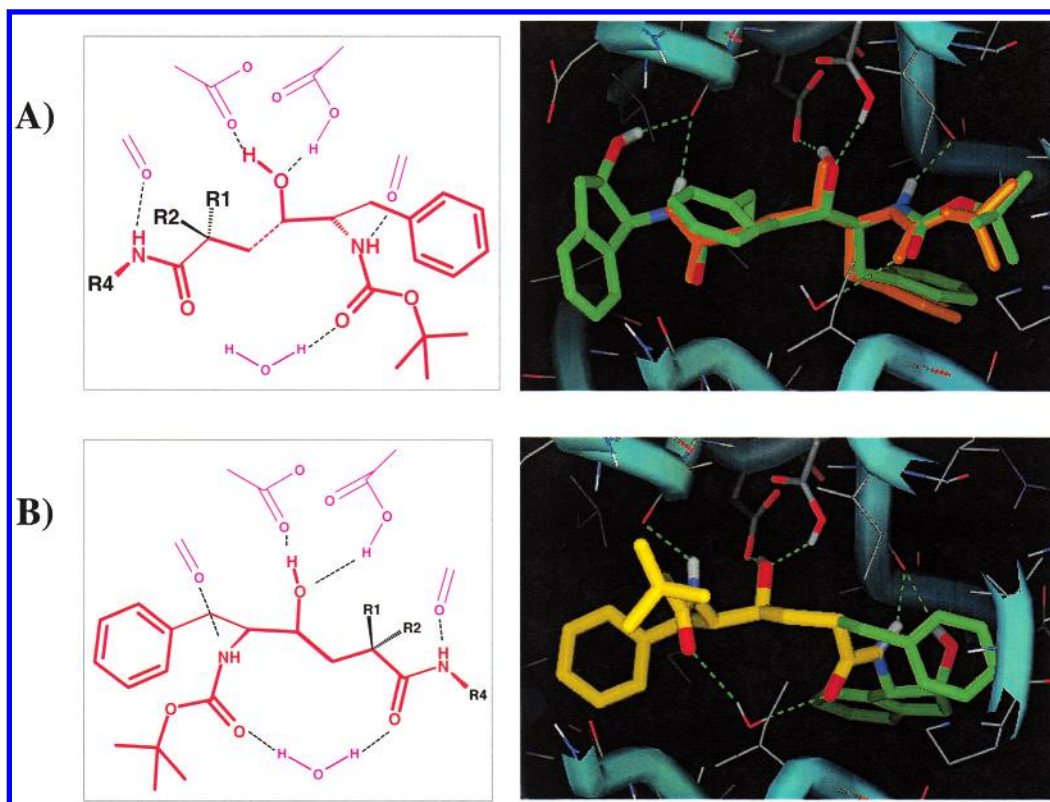
where  $r$  and  $s$  denote two docking modes. A  $p$ -value is determined by comparing the statistic  $t^*$  with the values one may observe from a  $T$  distributed random variable. Extremely high or low values of the  $t^*$  statistic are unlikely to be due to chance alone and thus give strong support to the hypothesis that the two means are different. A  $p$ -value less than 0.05 is often taken to indicate that the means are significantly different.

There is one difficulty with the use of the  $t$ -test in the above setting. The  $t$ -test assumes that the values realized are independent and identically distributed, with common variance and possibly different means. The use of the  $t$ -test in this setting involves a violation of the assumption of independence, since the values of  $R^2$  are the result of models that are computed from training sets that are overlapping across the 50 iterations. For example, in iteration 1 a given observation will be predicted from a model trained on 75% of the data. In iteration 2, the same observation will be predicted from a different model trained on another 75% portion of the data. To the degree that the training sets overlap, the models will tend to give the same predictions and the resulting values of  $R^2$  will be correlated. The practical result of this is that the value of  $K$  in the equation for the  $t$  statistic is inflated and the true  $p$ -value may be higher than what is computed. However, if the  $p$ -value from the above procedure is very much lower than 0.05, then the true  $p$ -value will also be below 0.05. Adjusting the statistic to properly reflect this dependence is a topic for further research.

## Results

We apply the described methodology to two literature data sets. The first data set of hydroxyethylenes tar-





**Figure 3.** Two-dimensional (left-hand side) and three-dimensional (right-hand side) representation of the docking modes. For the two-dimensional pictures the CS is shown in red, the protein atoms are shown in magenta, and the hydrogen bonds are depicted as black dotted lines. For the three-dimensional pictures the protein backbone is represented as a cyan tube, carbons of the inhibitors R-groups are green, CS atoms are orange for mode 1 and yellow for mode 2, nitrogens are blue, oxygens are red, protein carbons are gray, and hydrogen bonds are represented as dotted green lines: (A) mode 1; (B) mode 2 that is consistent with X-ray structure.

geted as HIV protease inhibitors<sup>1</sup> is widely accepted in the literature as a benchmark to test structure-based QSAR methodologies and descriptors.<sup>12,36</sup> The set of coordinates for the protein and inhibitors was kindly supplied to us by Kate Holloway. The X-ray structure of HIV-1 protease in a complex with L-689,502 including the bound water molecule was used for docking. Active site aspartic acid of the first chain was protonated. The set of supplied coordinates was used to evaluate the automated docking results. It is possible that the procedure is optimistically biased toward a success, if the HIV-1 from the complex contains the ligand shape imprinted in itself thus favoring the true binding mode. To avoid this putative shape and electrostatic bias, we also repeat the entire protocol with the native HIV-1 protease with open flaps and no bound water molecule (PDB code 3phv).<sup>37</sup> The chemical series with CS highlighted is shown in Table 1. Following Perez<sup>12</sup> we used compounds **1**, **3–29**, and **31–34** for our analysis with the expectation that this data set should be able to generate predictive models.

The second data set includes 53 oxoindoles with cellular IC<sub>50</sub> data in VEGF receptor tyrosine kinase assay.<sup>2</sup> The chemical series is represented in Table 2 with CS highlighted in blue. In this case the absence of X-ray structure at the time of the study necessitated the use of a homology model. We deliberately included a data set that has several approximations to show a range of situations that might occur in problems faced in the pharmaceutical industry.

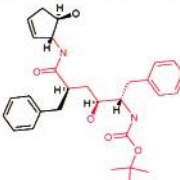
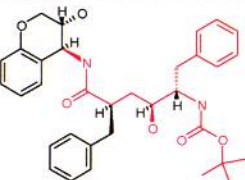
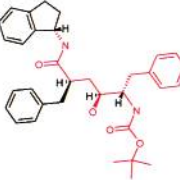
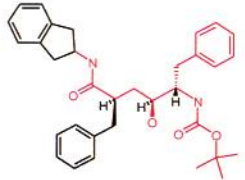
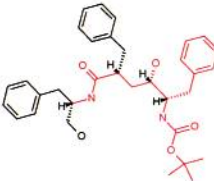
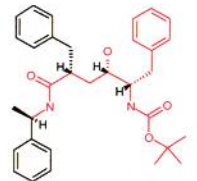
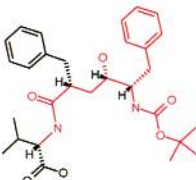
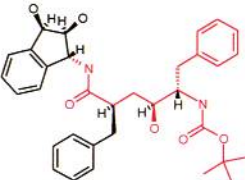
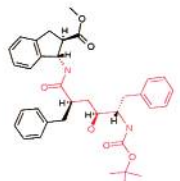
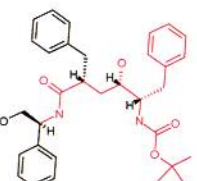
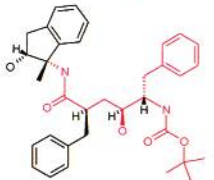
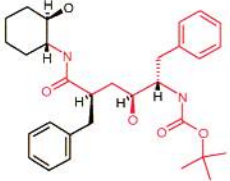
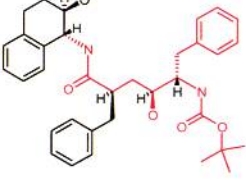
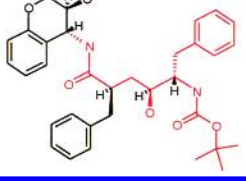
**HIV-1 Protease Inhibitor Data Set/Protein from HIV-1/L-689,502 Complex.** For this data set, the coordinates of the crystallographically determined hydroxy  $\alpha$ -carbon atom were defined as the center of the active site. Each of the 32 molecules in the chemical series was subjected to the multiple copy simultaneous sampling (MCSS)<sup>38</sup>-based annealing involving 20 replicas.<sup>14,23</sup> For each ligand the rms-based Ward's clustering was used to remove redundant docking solutions. The clustering of the resulting CS (shown in red in Figure 2A) revealed the existence of 12 significant clusters that are represented in Table 3. We chose to analyze in detail two major docking modes corresponding to the two most populated clusters. The two- and three-dimensional representations of the chosen docking modes are depicted in Figure 3A,B. In practice, it may be necessary to perform an analysis of more than two modes. For each MDM the entire series was redocked with NOE restraints for all CS atoms with four ligand replicas following the same annealing protocol. The top portion of Figure 4 shows the distribution of cross-validated  $R^2$  from the 4-fold cross-validations for the top two MDMs. The  $t$ -test shows that mode 2 is more predictive than mode 1. Thus we are convinced that the mode corresponding to the crystallographic complex is more consistent with the SAR. The mean value of the cross-validated  $R^2$  is 0.44. Analysis of individual descriptors revealed that the electrostatic contribution is poorly correlated with pIC<sub>50</sub>. In addition, examination of the automatically docked structures showed that the

**Table 1.** HIV-1 Protease Inhibitor Set<sup>a</sup>

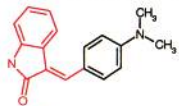
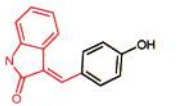
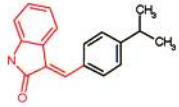
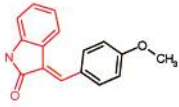
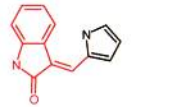
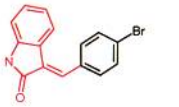
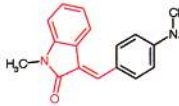
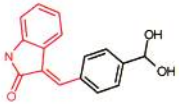
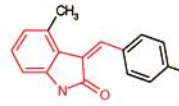
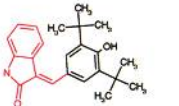
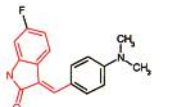
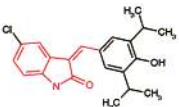

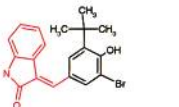
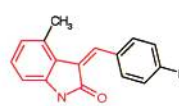
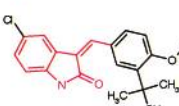

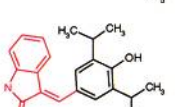
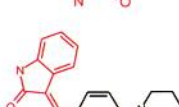
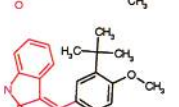
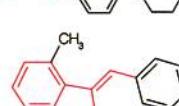
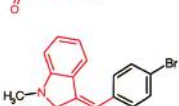
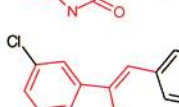
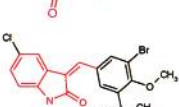
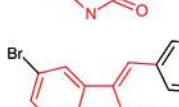
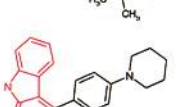
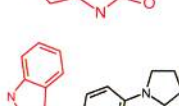
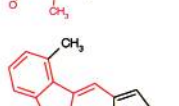

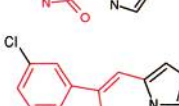
Name	Structure	pIC <sub>50</sub>	Name	Structure	pIC <sub>50</sub>
1		9.602	11		5.532
3		8.113	12		9.796
4		9.721	13		7.561
5		9.585	14		9.143
6		9.638	15		8.266
7		9.222	16		9.276
8		9.538	17		9.602
9		9.509	18		9.77
10		9.569	19		6.943

<sup>a</sup> pIC<sub>50</sub> is the negative log of IC<sub>50</sub>.

Table 1. (Continued)

Name	Structure	pIC50	Name	Structure	pIC50
20		8.021	29		7.392
21		7.465	31		6.886
22		6.161	32		6.836
23		6.793	33		10
24		7.179	34		7.413
25		6.673			
26		6.914			
27		9.155			
28		9.745			

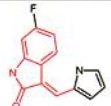
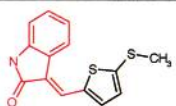
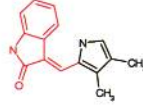
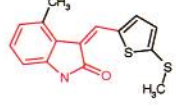
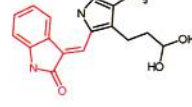
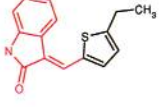
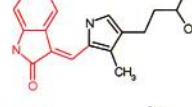
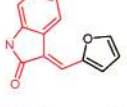
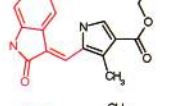
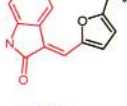
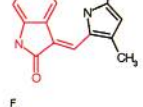
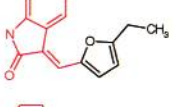
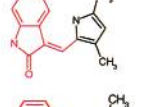
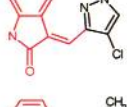
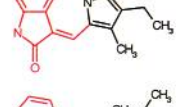
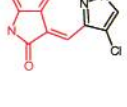
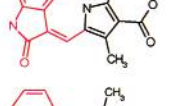
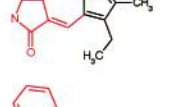
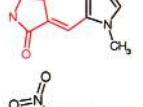
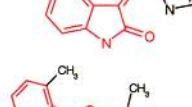
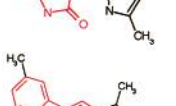
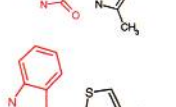

**Table 2.** VEGF Kinase Inhibitor Set<sup>a</sup>

Name	Structure	pIC <sub>50</sub>	Name	Structure	pIC <sub>50</sub>
1		6.10	25		5.57
2		5.28	26		5.12
3		6.41	27		3.00
13		4.65	28		3.00
14		5.52	29		5.08
15		5.34	30		5.37
16		5.29	31		4.33
17		5.60	32		3.00
18		4.00	33		5.07
19		5.60	34		3.00
20		5.68	35		3.00
21		5.39	36		3.00
22		4.30	37		3.00
23		5.52	38		4.51
24		5.35	39		5.52

<sup>a</sup> pIC<sub>50</sub> is the negative log of cellular IC<sub>50</sub>.



Table 2. (Continued)

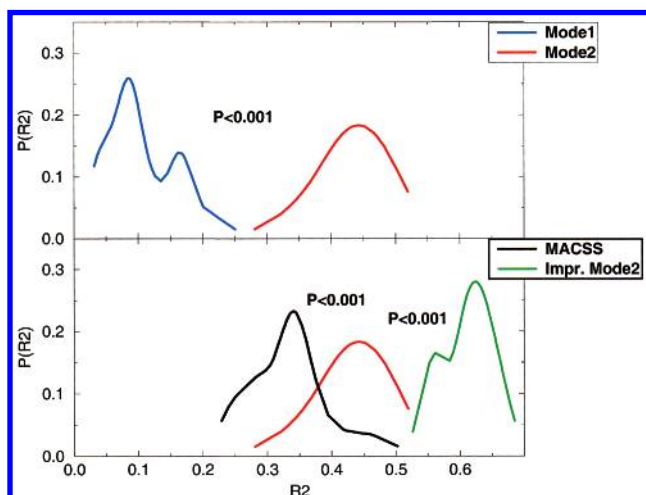
Name	Structure	pIC50	Name	Structure	pIC50
40		6.15	56		5.63
41		5.57	57		3.00
42		6.40	58		5.47
43		5.20	59		3.00
44		6.74	60		4.13
45		5.98	61		4.39
46		6.15	62		5.13
47		3.00	63		3.00
48		7.15			
49		6.85			
50		4.69			
51		3.00			
52		6.00			
53		6.52			
55		3.00			



**Table 3.** CS Clusters from an Unbiased Docking to HIV-1/L-689,502

cluster rank/ mode no.	cluster population <sup>a</sup>	Z score <sup>b</sup>	rms of the CS reference/X-ray <sup>c</sup>
1	20	10.45	7.26
2	15	7.64	1.18
3	12	5.95	7.25
4	11	5.39	8.22
5	9	4.26	7.97
6	9	4.26	7.07
7	8	3.70	7.46
8	6	2.58	6.25
9	5	2.01	8.29
10	5	2.01	8.28
11	5	2.01	7.14
12	4	1.45	4.54
13	3	0.89	6.13
14	3	0.89	5.44
15	3	0.89	7.57

<sup>a</sup> Cluster population refers to the number of CS from the docking simulations of entire molecules that belong to a given cluster. For example, a population of 20 for mode 1 means that 20 out of 32 series members exhibit this docking mode. <sup>b</sup> Z score<sup>35</sup> represents the normalized population of a cluster. For this data set Z scores greater than 2.0 could be considered significant. <sup>c</sup> Average of all heavy atom rms is shown for the CS between the cluster center and the supplied positions for the reference compounds.<sup>1</sup>



**Figure 4.** Distribution of the 50 predictive  $R^2$  values. The descriptor sets use the same data splits for each of the 50 trials. (Top) The mode 1 distribution is shown in blue. The mean value of  $R^2$  is 0.14. The mode 2  $R^2$  distribution is shown in red with the mean at 0.44. The  $p$ -value indicates that mode 2 is more predictive. (Bottom) The MACCS keys predictive  $R^2$  distribution is shown in black with a mean of 0.33. The improved mode 2 (by manual intervention to restrain hydrogen bonds across the series)  $R^2$  distribution is shown in green with a mean of 0.62. The  $p$ -values indicate that the improved mode 2 is more predictive than mode 2, which is more predictive than MACCS keys.

six CS hydrogen bonds for mode 2 are not preserved across the entire series. Further redocking using identical annealing schedule with additional restraints for all six hydrogen bonds led to a refined mode 2. The mean value of the cross-validated  $R^2$  for the improved mode 2 is 0.62. This value is similar to the leave-one-out  $R^2$  reported by Merck researchers after performing manual modeling of all structures. It is possible that more manual intervention of the final docked solution could further improve the predictability of the model. It is our belief, however, that the “average” modeler can obtain predictive models without much manual intervention. The bottom of Figure 4 shows the comparison of the

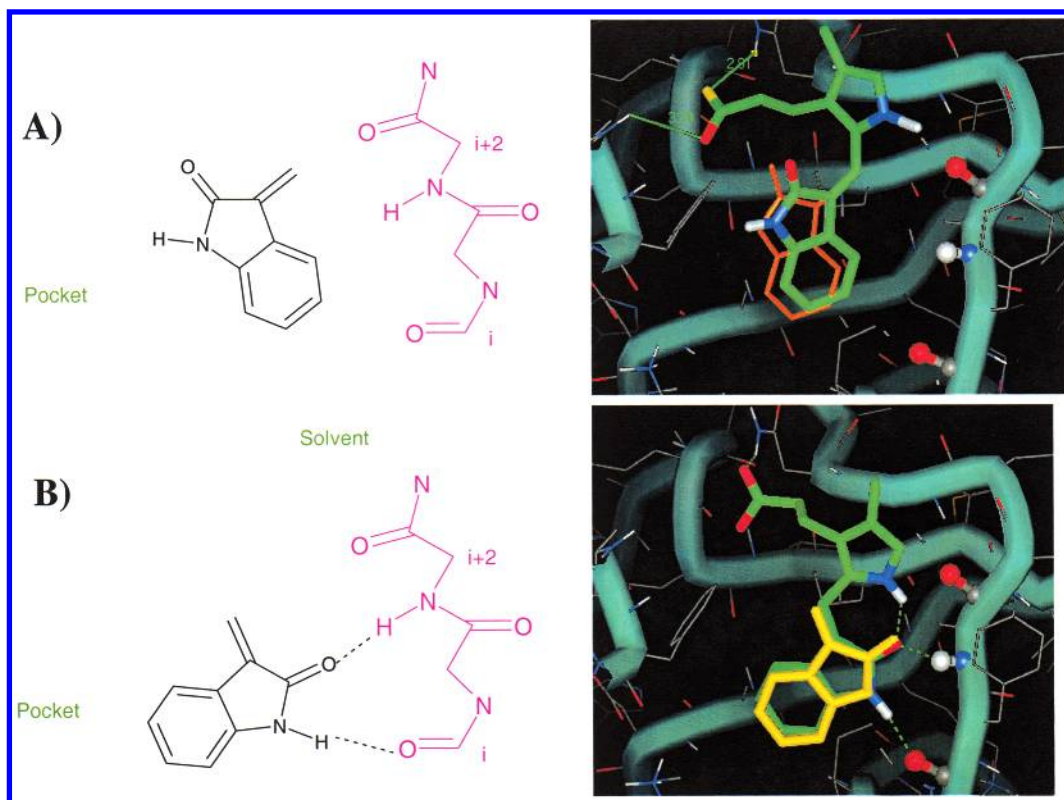
distribution of the cross-validated  $R^2$  for the improved mode 2 with the distribution for the fully automated mode 2.

How do the dock-derived QSAR models compare with two-dimensional QSAR models? To address this question, models were derived from identical 50 sets of train/test splits of the data using 166 MACCS keys<sup>39,40</sup> as descriptors. The bottom portion of Figure 5 shows that the mean  $R^2$  for the MACCS keys of 0.33 is significantly lower than that for mode 2 ( $p$ -value < 0.005). However, the MACCS keys show better predictive power than mode 1 of docking. These results suggest that MACCS keys can be used in general to indicate the lower bound of predictability that is expected from more sophisticated three-dimensional-based approaches. It is worth noting that the improved mode 2 provides a very predictive model that can be applied to prioritize synthesis of new analogues and evaluate novel ideas. Thus, DoMCoSAR demonstrates the interrelationship between docking mode and SAR: SAR can be helpful in determining the binding mode, and in turn a good binding mode can be used to create predictive models.

#### HIV-1 Protease Data Set/Native HIV-1 Protein.

One possible drawback of the above results could be a possible bias caused by the use of the “almost perfect” protein model. We did, after all, use the protein cocrystallized with one member of the series. The protein could likely contain the information about the shape of the entire series. To avoid this possible bias we have repeated the entire protocol, but this time the native HIV-1 protease structure was used. As in the example above the active site Asp of the first chain was protonated. The native protein structure is slightly different in the active site especially in the flap region. The open conformation is likely to influence the interaction of the entire series with flaps. Despite this, the reported results suggest that one can obtain predictive models for the series even with the native protein, if the same ligand coordinates as for HIV-1/L-689,502 are used.<sup>1</sup> However, it remains unclear whether an automated approach could provide the geometry of the inhibitors required to build predictive models if only the native protein were available.

The entire series of 32 ligands was automatically docked to the native HIV-1 protease. Clustering of CS revealed the two most populated MDMs. In this case the most populated cluster corresponds to the true solution. The second CS docking mode represents the inverted true solution just as in the case of the L-689,502-inhibited enzyme. Table 4 shows the detailed results of the CS clustering. The center of the major cluster corresponding to the true solution in the native HIV-1 is on average a little more distant from the reference structures than the CS of true solution in the HIV-1/L-689,502 complex. For the two native protein MDMs the entire series of 32 ligands was redocked with restraints to the CS positions and four conserved CS hydrogen bonds to the protein. For each docking mode, four docking-based descriptors were generated for each ligand. In this case 50 4-fold cross-validations revealed that the true docking mode has a mean  $R^2$  of 0.40 which is significantly better than the mean  $R^2$  of 0.19 for the inverted docking mode ( $p$ -value < 0.005). The QSARs resulting from the docking to the native HIV-1 protease



**Figure 5.** Two-dimensional (left-hand side) and three-dimensional (right-hand side) representation of the docking modes. For the two-dimensional pictures the CS is shown in red, the protein atoms are shown in magenta, and the hydrogen bonds are depicted as black dotted lines. For three-dimensional pictures the protein backbone is represented as a cyan tube, carbons of inhibitors R-groups are green, CS atoms are orange for mode 1 and yellow for mode 2, nitrogens are blue, oxygens are red, protein carbons are gray, and hydrogen bonds are represented as dotted green lines: (A) mode 1; (B) mode 2 that is consistent with X-ray structure.

**Table 4.** CS Clusters for an Unbiased Docking to the Native HIV-1 Protease<sup>37</sup>

cluster rank/ mode no.	cluster population <sup>a</sup>	Z score <sup>b</sup>	rms of the CS reference/X-ray <sup>c</sup>
1	16	15.17	1.51
2	14	13.13	8.36
3	7	5.99	8.45
4	6	4.97	8.00
5	4	2.93	8.73
6	4	2.93	7.71
7	4	2.93	9.18
8	3	1.91	5.14
9	3	1.91	1.78
10	3	1.91	6.85
11	2	0.89	6.87
12	2	0.89	6.92
13	2	0.89	7.38
14	2	0.89	8.33
15	2	0.89	8.66

<sup>a-c</sup> See corresponding footnotes in Table 3.

are thus less predictive than those obtained with the L-689,502-inhibited enzyme. Even so, it is impressive to obtain a result that is significantly better than random even under somewhat less than optimal conditions. It is also of interest to note that using different ligand charge assignment methods can in many cases alter the predictability of both QSAR models. Starting from the final structures generated by DoMCoSAR, we examined five charge assignment methods available in Insight 97.5<sup>27</sup> In each case DoMCoSAR structures were minimized with 500 steps of conjugate gradient to allow for slight adjustments. The results are reported in Table 5. Ironically, the more involved ab initio charges provide

less predictive models than those with charges generated with Insight in a matter of seconds. We also noted that the use of strain energy does not add to the predictability of the models for Insight-generated ligand charges. Most predictive models (as judged by 50 4-fold cross-validation results) can be obtained with cff91 Insight charges for the native HIV-1 complexes. However, for the L-689,502-inhibited protein the Insight-generated Amber charges provide the most predictive model with the average  $R^2$  of 0.73. In all cases the L-689,502-docked complexes give significantly more predictive models than the native protein complexes. Thus the quality of the QSAR models seems to strongly correlate with the quality of the protein model. However, the important finding is that for this SAR, DoMCoSAR can use even the uncomplexed protein as basis to construct predictive and interpretable models.

**Oxoindole Data Set.** To test the generality of the approach and to identify possible limitations, we applied DoMCoSAR to a set of 53 oxoindoles targeted at tyrosine kinases. The entire series used in this study is depicted in Table 2 with CS highlighted in red. IC<sub>50</sub> data come from a cell-based assay. We did not have access to the crystallographically determined coordinates of VEGF RTK-1 for which the oxoindoles show the best inhibitory effect; however, two publicly available X-ray structures of the oxoindole series with FGF tyrosine kinase (PDB codes 1agw and 1fgi<sup>41</sup>) were available. FGFR kinase shares 44% sequence identity with VEGF kinase. The PSI-Blast<sup>42</sup> sequence alignment and MODELER<sup>43</sup> pack-

**Table 5.** Comparison of DoMCoSAR QSARs for Different Ligand Charge Assignments and Different Proteins

ligand charge <sup>a</sup>	protein <sup>b</sup>	$R^2$ <sup>c</sup>	leave-one-out $R^2$ <sup>d</sup>	4-way cross-validated $R^2$ <sup>e</sup>	weights for terms, pIC <sub>50</sub> <sup>f</sup>
6-31G*	native	0.55	0.41	0.40 ± 0.041	−3.1 − 0.25Elec − 0.15VdW + 0.03Eis + 1.17Strain
4 descriptors		(0.38)	(0.20)	(0.19 ± 0.051)	
6-31G*	native	0.49	0.34	0.34 ± 0.047	−6.8 − 0.37Elec − 0.24VdW + 0.06Eis
3 descriptors		(0.39)	(0.22)	(0.22 ± 0.059)	
Quanta template	native	0.61	0.46	0.46 ± 0.049	−7.8 − 0.42Elec − 0.28VdW + 0.06Eis
		(0.33)	(0.15)	(0.15 ± 0.055)	
cvff	native	0.62	0.46	0.45 ± 0.043	−5.7 − 0.46Elec − 0.22VdW + 0.05Eis
		(0.37)	(0.18)	(0.19 ± 0.060)	
cvff91	native	0.66	0.53	0.52 ± 0.040	−6.8 − 0.44Elec − 0.22VdW + 0.04Eis
		(0.38)	(0.14)	(0.15 ± 0.053)	
Amber	native	0.59	0.48	0.46 ± 0.039	−4.4 − 0.29Elec − 0.25VdW + 0.05Eis
		(0.37)	(0.20)	(0.20 ± 0.054)	
6-31G*	L689-502-inhibited	0.76	0.65	0.62 ± 0.056	−13.9 − 0.13Elec − 0.34VdW + 0.023Eis − 0.07Strain
4 descriptors					
6-31G*	L689-502-inhibited	0.76	0.71	0.69 ± 0.031	−15.1 − 0.17Elec − 0.34VdW + 0.003Eis
Quanta template	L689-502-inhibited	0.76	0.71	0.70 ± 0.027	−14.2 − 0.17Elec − 0.33VdW − 0.004Eis
cvff	L689-502-inhibited	0.78	0.72	0.70 ± 0.030	−13.4 − 0.20Elec − 0.31VdW + 0.0001Eis
cvff91	L689-502-inhibited	0.76	0.69	0.68 ± 0.027	−14.5 − 0.18Elec − 0.32VdW + 0.001Eis
Amber	L689-502-inhibited	0.78	0.73	0.73 ± 0.024	−12.1 − 0.11Elec − 0.33VdW − 0.005Eis

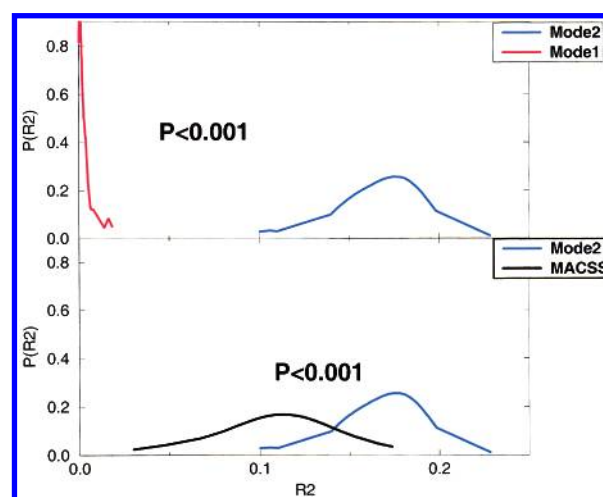
<sup>a</sup> Ligand charges were generated using Insight 97.5,<sup>27</sup> except 6-31G\* which were generated with Gaussian.<sup>26</sup> All ligands had formal charge of 0. Protein polar hydrogen representation with CHARMM PARAM19/TOPH19 topology and parameter files<sup>22</sup> were used in all calculations. <sup>b</sup> Protein structure used for dockings and descriptor calculations. <sup>c</sup> Correlation coefficients  $R^2$  for all 32 ligands. For the native HIV-1 protease the numbers in parentheses refer to the inverted/"nonnative" docking mode. <sup>d</sup> Squared correlation coefficient resulting from leave-one-out cross-validation. For the native HIV-1 protease the numbers in parentheses refer to the inverted/"nonnative" docking mode. <sup>e</sup> Average squared correlation coefficient resulting from 50 4-fold cross-validation experiments. Standard deviations are also reported, which can be used in conjunction with eq 5 to compute  $t$  statistics. For the native HIV-1 protease the numbers in parentheses refer to the inverted/"nonnative" docking mode. In all cases the true docking mode produces significantly better QSAR models than the inverted mode. The 6-31G\* with 3 descriptors is the only QSAR model that is not significantly better than two-dimensional MACCS QSAR. Gaussian-generated charges do not produce the most predictive models; more predictive models can be constructed if cvff91 or Amber charges on ligands are used for the native and L-689-502-inhibited HIV-1 protease, respectively. For all cases except the native HIV-1 protease with 6-31G\* ligand charges, 3-descriptor models are significantly more predictive than 4-descriptor models. <sup>f</sup> The resulting equation for the  $-\log(\text{IC}_{50})$  for all 32 ligands for the X-ray-like docking mode. Elec denotes electrostatic ligand and ligand-protein interaction energy; VdW denotes the van der Waals ligand and ligand protein interaction energy; Eis denotes the surface-based Eisenberg solvation energy; Strain denotes ligand's strain energy. Note that the weightings are not indicative of the importance of the descriptors. van der Waals energies are most correlated with activities in all cases with leave-one-out  $R^2$  ranging from 0.3 (6-31G\* ligand charges with native protein) to 0.68 (Amber ligand charges and L-689-502-inhibited protein).

**Table 6.** CS Clusters for an Unbiased Docking of Oxindole Series to VEGF Model

cluster rank	cluster population	Z score	rms of the CS from X-ray <sup>41</sup>
1	37	7.50	3.12
2	32	6.42	0.55
3	21	4.03	6.36
4	17	3.17	9.00
5	13	2.30	8.48
6	12	2.08	5.48
7	11	1.87	8.00
8	8	1.22	6.81
9	8	1.22	3.89
10	8	1.22	5.25
11	7	1.00	4.01
12	6	0.78	6.87
13	5	0.56	8.05
14	4	0.35	6.08
15	4	0.35	1.77

age were used to generate a model of VEGF kinase based on 1fgi.<sup>41</sup> No water molecules were retained.

Unbiased docking and clustering revealed 11 major binding modes (Table 6). The pictorial representation of two modes is shown in Figure 5A,B. As was done with the HIV-1 protease test case, we have chosen the two most significantly populated modes to evaluate in 50 trials of 4-fold cross-validation. The distribution of predictive  $R^2$  values for two modes is shown in the top portion of Figure 6. The entire distributions are well-separated as well as the means ( $p$ -value < 0.005); however, the mean  $R^2$  of the more predictive set is still below 0.2. The bottom portion of Figure 6 reveals that



**Figure 6.** Distribution of the 50 predictive  $R^2$  values. All data splits are identical for all descriptor sets. (Top) The mode 1 distribution is shown in blue. The mean value of  $R^2$  is 0.01. The mode 2  $R^2$  distribution is shown in red with a mean of 0.15. The  $p$ -value indicates that mode 2 is more predictive. (Bottom) The MACCS keys predictive  $R^2$  distribution is shown in black with a mean of 0.05.<sup>12</sup>

models from MACCS key descriptors also perform poorly in cross-validation for this data set. The fact that both three-dimensional docking and two-dimensional MACCS keys are unable to build predictive models suggests numerous complications. One may conjecture that such behavior could result from attempting to build models based on cellular assay data, since there could be factors



differentially affecting permeability and selectivity of the compounds. This conjecture appears to be partially supported by the recent enzyme VEGF assay data for 22 members of the series which shows no correlation with VEGF cellular data.<sup>44</sup> Another possible explanation is that multiple binding modes could occur, thus violating the primary assumption of this work and making the series difficult for traditional QSAR methods to handle. This is a topic of current research. Another significant factor contributing to poor predictability of the docking modes could be related to the fact that the homology model may not well represent the true protein. We note that our homology model matched the ATP binding site of the recently disclosed VEGF X-ray structure<sup>45</sup> very well; thus the protein modeling is less likely to be the cause of the poor QSAR models in this case. However, despite the poor predictive value of the model, it is the docking mode that is consistent with the X-ray structures of the two kinases that has the superior cross-validation profile. For this series, even though we were unable to create a good predictive model, DoMCoSAR was able to identify the binding mode consistent with X-ray structures of related complexes.

## Conclusions

We have demonstrated that for a chemical series, DoMCoSAR can be helpful to statistically validate and discriminate between possible docking modes. The application of *t*-tests to the docking mode-dependent predictive  $R^2$  is a novel way to address the question of docking mode SAR consistency. For the two cases examined here, DoMCoSAR indicates that the docking mode consistent with the X-ray structure of the complex produces a QSAR model with higher predictive power than QSARs derived from other modes. For some chemical series, building docking-based predictive models is possible, but it is difficult to generalize this statement. We found that the quality of the protein model influences the predictability of the QSARs. For the series of HIV-1 protease inhibitors, we demonstrated that true binding mode could be identified using the uncomplexed enzyme and serves to build predictive models. However the use of the complexed HIV-1 protein with the bound water molecule did provide significantly better models. As observed for the oxindole series, highly predictive docking-based models could not be created despite the undeniable value of generating the hypothetical binding mode. In addition we have postulated that models derived from MACCS keys or other two-dimensional descriptors can be effectively used to estimate the lower bound of series' predictive ability.

This work gives supporting evidence that docking can be extremely helpful to medicinal chemistry lead optimization efforts. However, we feel that the utility of docking as a virtual screening tool needs to be carefully examined. As we have demonstrated, only about 50% of the molecules of the series exhibit the unbiased docking mode that is consistent with the X-ray structure. Thus, docking of databases carries a danger that the score for some molecules will be evaluated based on the incorrect binding mode. This is especially true for the receptors that undergo conformational rear-

angement upon binding. We will address the question of scoring of database-docked structures in an upcoming report.

**Acknowledgment.** We thank Kate Holloway from Merck Research Laboratories for sending us the modeled structures of HIV-1 protease inhibitors and very insightful comments. We also thank referees of the manuscript whose comments vastly improved the quality of the presented work. We are grateful to Bernard Brooks for providing valuable suggestions for the functional form of the docking potential. We thank Dr. Jon Erickson for useful comments and suggestions. Helpful discussions with Angel Ortiz, Charlie Brooks, Richard Higgs, Robert Babine, Jim Wikel, and Jean-Pierre Wery are appreciated.

## References

- Holloway, K. M.; Wai, J. M.; Halgren, T. A.; Fitzgerald, P. M. D.; Vacca, J. P.; Dorsey, B. D.; Levin, R. B.; Wayne, J. T.; Chen, L. J.; deSolms, J. S.; Gaffin, N.; Ghosh, A. K.; Giuliani, E. A.; Graham, S. L.; Guare, J. P.; Hungate, R. W.; Lyle, T. A.; Sanders, W. M.; Tucker, T. J.; Wiggins, M.; Wiscount, C. M.; Woltersdorf, O. W.; Young, S. D.; Darke, P. L.; Zugay, J. A. A Priori Prediction of Activity for HIV-1 Protease Inhibitors Employing Energy Minimization in the Active Site. *J. Med. Chem.* **1995**, *38*, 305–317.
- Sun, L.; Tran, N.; Tang, F.; App, H.; Hirth, P.; McMahon, G.; Tang, C. Synthesis and Biological Evaluations of 3-Substituted Indolin-2-ones: A Novel Class of Tyrosine Kinase Inhibitors that Exhibit Selectivity toward Particular Receptor Tyrosine Kinases. *J. Med. Chem.* **1998**, *41*, 2588–2603.
- Gallop, M. A.; Barret, R. W.; Dower, W. J.; Fodor, S. P. A.; Gordon, E. M. Applications of combinatorial technologies to drug discovery. 1. Background and peptide combinatorial libraries. *J. Med. Chem.* **1994**, *37*, 1233–1251.
- Gordon, E. M.; Barret, R. W.; Dower, W. J.; Fodor, S. P.; Gallop, M. A. Applications of combinatorial technologies to drug discovery. 2. Combinatorial organic synthesis, library screening strategies, and future directions. *J. Med. Chem.* **1994**, *37*, 1385–401.
- Zheng, Q.; Kyle, D. J. Computational screening of combinatorial libraries. *Bioorg. Med. Chem.* **1996**, *4*, 631–638.
- Muegge, I.; Martin, Y. C.; Hajduk, P. J.; Fesik, S. W. Evaluation of PMF scoring in docking weak ligands to the FK506 binding protein. *J. Med. Chem.* **1999**, *42*, 2498–503.
- Stewart, K. D.; Bentley, J. A.; Cory, M. DOCKing ligands into receptors: The test case of A-Chymotrypsin. *Tetrahedron Comput. Methodol.* **1990**, *3*, 713–722.
- Charifson, P. S.; Corkery, J. J.; Murcko, M. A.; Walters, P. W. Consensus Scoring: A Method for Obtaining Improved Hit Rates from Docking Databases of Three-Dimensional Structures into Proteins. *J. Med. Chem.* **1999**, *42*, 5100–5109.
- Fisher, E.; Thierfelder, H. *Chem. Ber.* **1894**, *27*, 2031.
- Kuntz, I. D.; Blaney, J. M.; Oatley, S. J.; Langridge, R.; Ferrin, T. E. A geometric approach to macromolecule-ligand interactions. *J. Mol. Biol.* **1982**, *161*, 269–288.
- Gschwend, D. A.; Good, A. C.; Kuntz, I. D. Molecular Docking Towards Drug Discovery. *J. Mol. Recognit.* **1996**, *9*, 175–186.
- Perez, C.; M. P.; Ortiz, A.; Gago, F. Comparative Binding Energy Analysis of HIV-1 Protease Inhibitors: Incorporation of Solvent Effects and Validation as a Powerful Toll in Receptor-Based Drug Design. *J. Med. Chem.* **1998**, *41*, 836–852.
- Jalaie, M.; Erickson, J. A. Homology Model Directed Alignment Selection for Comparative Molecular Field Analysis: Application to Photosystem II Inhibitors. *J. Comput.-Aided Mol. Des.* **2000**, *14*, 181–197.
- Vieth, M.; Hirst, J. D.; Dominy, B. N.; Daigler, H.; Brooks III, C. L. Assessing Search Strategies for Flexible Docking. *J. Comput. Chem.* **1998**, *19*, 1623–1631.
- Judson, R. S.; Tan, Y. T.; Mori, E.; Melius, C.; Jeager, E. P.; Treasurywala, A. M.; Mathiowetz, A. Docking flexible molecules: A case study of three proteins. *J. Comput. Chem.* **1995**, *16*, 1405–1419.
- Jones, G.; Willet, P. Docking of small-molecule ligands into active sites. *Curr. Opin. Biotechnol.* **1995**, *6*, 652–656.
- Goodsel, D. S.; Olson, A. J. Automated docking of substrates to proteins by simulated annealing. *Proteins* **1990**, *8*, 195–202.
- Goldsmith, E. J.; Cobb, M. H. Protein kinases. *Curr. Opin. Struct. Biol.* **1994**, *4*, 833–840.

- (19) Wilson, K. P.; McCaffrey, P. G.; Hsiao, K.; Pazhanisamy, S.; Galullo, V.; Bemis, G. W.; Fitzgibbon, M. J.; Caron, P. R.; Murcko, M. A.; Su, M. S. S. The structural basis for the specificity of pyridinylimidazole inhibitors of p38 MAP kinase. *Chem. Biol.* **1997**, *4*, 423–431.
- (20) Jones, T. A.; Kleywegt, G. J. CASP3 Comparative Modeling Evaluation. *Proteins: Struct. Funct. Genet. Suppl.* **1999**, *3*, 30–46.
- (21) Bates, P. A.; Sternberg, M. J. E. Model Building by Comparison at CASP3: Using Expert Knowledge and Computer Automation. *Proteins: Struct. Funct. Genet. Suppl.* **1999**, *3*, 47–54.
- (22) Brooks, B. R.; Brucoleri, R. E.; Olafson, B. D.; States, D. J.; Swaminathan, S.; Karplus, M. CHARMM: A program for macromolecular energy, minimization and dynamics calculations. *J. Comput. Chem.* **1983**, *4*, 187–217.
- (23) Vieth, M.; Hirst, J. D.; Kolinski, A.; Brooks III, C. L. Assessing Energy Functions for Flexible Docking. *J. Comput. Chem.* **1998**, *19*, 1612–1622.
- (24) Brooks, B. Personal communication.
- (25) QUANTA, 4.6 ed.; Molecular Simulations Inc.: San Diego, CA, 1997.
- (26) Frisch, M. J.; Trucks, G. W.; Schlegel, H. B.; Gill, P. M.; Johnson, B. G.; Robb, M. A.; Cheeseman, J. R.; Keith, T.; Petersson, G. A.; Montgomery, J. A.; Raghavavachari, K.; Al-Laham, M. A.; Zakrzewski, A. G.; Ortiz, J. V.; Foresman, J. B.; Cioslowski, J.; Stefanov, B. B.; Nanayakkara, A.; Challacombe, M.; Peng, C. Y.; Ayala, P. Y.; Chen, W.; Wong, M. W.; Anders, J. L.; Replogle, E. S.; Gomperts, R.; Martin, R. L.; Fox, D. J.; Binkley, J. S.; Defrees, D. J.; Baker, J.; Stewart, J. P.; Head-Gordon, M.; Gonzales, C.; Pople, J. A. *Gaussian 94*; Gaussian, Inc.: Pittsburgh, PA, 1995.
- (27) *Insight II*, release 97.5; Molecular Simulations Inc.: San Diego, CA, 1998.
- (28) Jain, A. K.; Dubes, R. C. *Algorithms for Clustering Data*; Prentice Hall: Englewood Cliffs, NJ, 1988.
- (29) Vieth, M.; Hirst, J. D.; Brooks, C. L., III. Do active site conformations of small ligands correspond to low free-energy solution structures? *J. Comput.-Aided Mol. Des.* **1998**, *12*, 563–572.
- (30) Wesson, L.; Eisenberg, D. Atomic solvation parameters applied to molecular dynamics of proteins in solution. *Protein Sci.* **1992**, *2*, 227–235.
- (31) Wold, H. *Soft Modelling*; Wold, H., Ed.; North-Holland: Amsterdam, 1981.
- (32) Wold, H. *Soft Modeling by Latent Variables; the Nonlinear Iterative Partial Least Squares Approach*; Wold, H., Ed.; Academic Press: London, 1975.
- (33) SAS; SAS Institute Inc.: Cary, NC, 1989–96.
- (34) Silverman, B. W. *Density Estimation for Statistics and Data Analysis*; Chapman & Hall: New York, London, 1986.
- (35) Bulmer, M. G. *Principles of Statistics*; Dover Publications: New York, 1979.
- (36) Muegge, I.; Martin, Y. C. A general and fast scoring function for protein–ligand interactions: a simplified potential approach. *J. Med. Chem.* **1999**, *42*, 791–804.
- (37) Lapatto, R.; Blundell, T.; Hemmings, A.; Overington, J.; Wilderspin, A.; Wood, S.; Merson, J. R.; Whittle, P. J.; Danley, D. E.; Geoghegan, K. F.; Hawrylik, S. J.; Lee, S. E.; Scheld, K. G.; Hobart, P. M. X-ray analysis of HIV-1 proteinase at 2.7 Å resolution confirms structural homology among retroviral enzymes. *Nature* **1989**, *342*, 299–302.
- (38) Miranker, A.; Karplus, M. Functionality maps of binding sites: A multiple copy simultaneous search method. *Proteins* **1991**, *11*, 29–34.
- (39) MACCS-II; Molecular Design Ltd.: San Leandro, CA.
- (40) Brown, R. D.; Martin, Y. C. The information content of 2D and 3D structural descriptors relevant to ligand–receptor binding. *J. Chem. Inf. Comput. Sci.* **1997**, *37*, 1–9.
- (41) Mohammadi, M.; McMahon, G.; Sun, L.; Tang, C.; Hirth, P.; Yeh, B. K.; Hubbard, S. R.; Schlessinger, J. Structures of the tyrosine kinase domain of fibroblast growth factor receptor in complex with inhibitors. *Science* **1997**, *276*, 955–960.
- (42) Altschul, S. F.; Madden, T. L.; Schaffer, A. A.; Zhang, J.; Zhang, Z.; Miller, W.; Lipman, D. J. Gapped BLAST and PSI-BLAST: a new generation of protein database search programs. *Nucleic Acid Res.* **1997**, *25*, 3389–3402.
- (43) Sali, A.; Blundell, T. L. Comparative protein modelling by satisfaction of spatial restraints. *J. Mol. Biol.* **1993**, *234*, 779–815.
- (44) Sun, L.; Tran, N.; Liang, C.; Tang, F.; Rice, A.; Schreck, R.; Waltz, K.; Shawver, L. K.; McMahon, G.; Tang, C. Design, Synthesis, and Evaluation of Substituted 3-[(3- or 4-Carboxyethylpyrrol-2-yl)methylidene]indoline-2-ones as Inhibitors of VEGF, FGF and PDGF Receptor Tyrosine Kinases. *J. Med. Chem.* **1999**, *42*, 5120–5130.
- (45) McTigue, M. A.; Wickersham, J.; Pinko, C.; Showalter, R.; Parast, C.; Tempczyk-Russell, A.; Gehring, M.; B. M.; Kan, C.; Villafraña, J.; Appelt, K. Crystal structure of the kinase domain of human vascular endothelial growth factor receptor 2: a key enzyme in angiogenesis. *Structure* **1999**, *7*, 319–330.

JM990609E